IET Microwaves, Antennas & Propagation

Research Article

Low specific absorption rate microstrip patch antenna for cellular phone applications

ISSN 1751-8725
Received on 22nd December 2014
Revised on 17th May 2015
Accepted on 12th June 2015
doi: 10.1049/iet-map.2014.0861
www.ietdl.org

Mohammad Rashed Iqbal Faruque[1], Md Ikbal Hossain[1] ✉, Mohammad Tariqul Islam[2]

[1]*Space Science Centre (ANGKASA), Research Centre Building, Universiti Kebangsaan Malaysia, UKM 43600, Bangi, Selangor D.E., Malaysia*

[2]*Department of Electrical, Electronic and Systems Engineering, Faculty of Engineering and Built Environment, Universiti Kebangsaan Malaysia, UKM 43600, Bangi, Selangor D.E., Malaysia*

✉ *E-mail: ipk_eee@yahoo.com*

Abstract: The aim of this study is to design a new microstrip-fed patch antenna for cell phone applications. The antenna design is composed of slots and Flame Retardant 4 dielectric substrate fed by a partial ground plane and a microstrip line. The user's effects on antenna performances are also analysed using standard specific anthropomorphic mannequin head phantom. The specific absorption rate (SAR) values of the proposed antenna are evaluated for different frequency bands considering cheek position of talk mode. The proposed antenna has an impedance bandwidth of 230.4 MHz (0.725–0.95 GHz, lower band), and 522.24 MHz (1.74–2.25 GHz, upper band), which can cover global system for mobile (GSM) 900 MHz, digital communication system 1800 MHz, personal communications service 1900 MHz, GSM 1900 MHz, and universal mobile telecommunications service 2100 MHz bands. Moreover, the proposed antenna produces lower SAR values in the human head than that of a dipole antenna, helical antenna, and planar inverted-F antenna.

1 Introduction

Nowadays, the cellular phones are indispensable part of our life. The most essential component of a cell phone is an antenna that transmits and receives electromagnetic (EM) waves. A few years ago, monopole antennas were used for mobile phone, which were large in size and provided single-frequency operation only. The first generation of mobile phone antenna was an external antenna, which was usually mounted on the top of a cell phone body. However, the recent trend is to use internal and planar antennas for handset devices. The mobile phone manufacturers now prefer low profile integrated antenna with high gain, high radiation efficiency, wide bandwidth, and multi-band behaviours. Microstrip patch antennas have become popular because of low cost, wideband abilities, and improved performances [1].

In the last decade, a wide variety of internal antennas has been proposed for the handset applications comprising planar inverted-F antenna (PIFA) [2], inverted-F antenna [3], folded chip [4] etc. In [5], an oval-shaped quad-band antenna was proposed for internal handset antenna. Moreover, different types of microstrip-patch antennas were also proposed in the literature for various applications. In [6], a dual-band folded loop microstrip-patch antenna was designed for wireless local area network (WLAN) applications. A microstrip-patch antenna was introduced for personal communications service (PCS) and Bluetooth application of mobile phone in [7]. In [8], a compact microstrip-patch antenna was designed for global positioning system and digital communication system (DCS) applications. Moreover, a multi-band microstrip-patch antenna was presented for global system for mobile (GSM), WLAN, and worldwide interoperability for microwave access (WiMAX) applications in [9]. In [10], another approach of triple-band patch antenna was proposed for PCS, WLAN, and WiMAX applications. In [11], a waveguide circular-slotted patch antenna was designed and fabricated for wireless fidelity, wireless internet (WiFi) and WiMAX applications. Recently, the biological effects of EM energy radiated from the cell phone antenna have attracted gusto in the research community as the EM radiation disturbs the biological system of human body [12]. As reported by the World Health Organization (WHO), radiation from mobile phone could cause cancer towards the public users [13]. To prevent the cell phone user from the EM exposure, safety limits are imposed usually in terms of specific absorption rate (SAR). International Commission on Non-Ionizing Radiation Protection and IEEE has imposed the limit of 2 W/kg (SAR) absorbed per 10 g of tissue [14, 15]. On the other hand, American National Standards Institute and Federal Communication Commission have defined the SAR limit to 1.6 W/kg per 1 g of body tissue [16]. Therefore, the antenna with the SAR is an essential issue for the cell phones and many researchers are working on this aspect.

Moreover, it should be ensured that the phones need to perform well under the real environment condition of the user holding the phone against his or her head as the human body can intervene with the operation of close-by antennas. The user proximity to the cell phone leads to negative effects on antenna performances involving impedance detuning, the resonance frequency shifting, and radiation efficiency degradation [17]. The other handset components including the battery, the camera, liquid crystal display (LCD) monitor, mobile casing etc. also affect the antenna performances [18].

In this paper, a new microstrip-patch antenna is presented for mobile phone applications that can be operated in the GSM, DCS, PCS, and universal mobile telecommunications service (UMTS) frequency bands. The antenna design is also focused on the effects of the user phantoms and other components on antenna performances. Moreover, the SAR values in the user's head are analysed and compared with other types of conventional antenna.

2 Antenna geometry

Fig. 1*a* shows the geometrical layout of the proposed microstrip-patch antenna. The designed antenna comprises a radiating element in one side of the substrate and a partial ground plane on the other side. The Flame Retardant 4 (FR-4) material is used as antenna substrate with relative permittivity (ε_r) 4.56, relative permeability (μ_r) 1, and loss tangent 0.02. The substrate thickness is 0.8 mm. The design specifications of the proposed

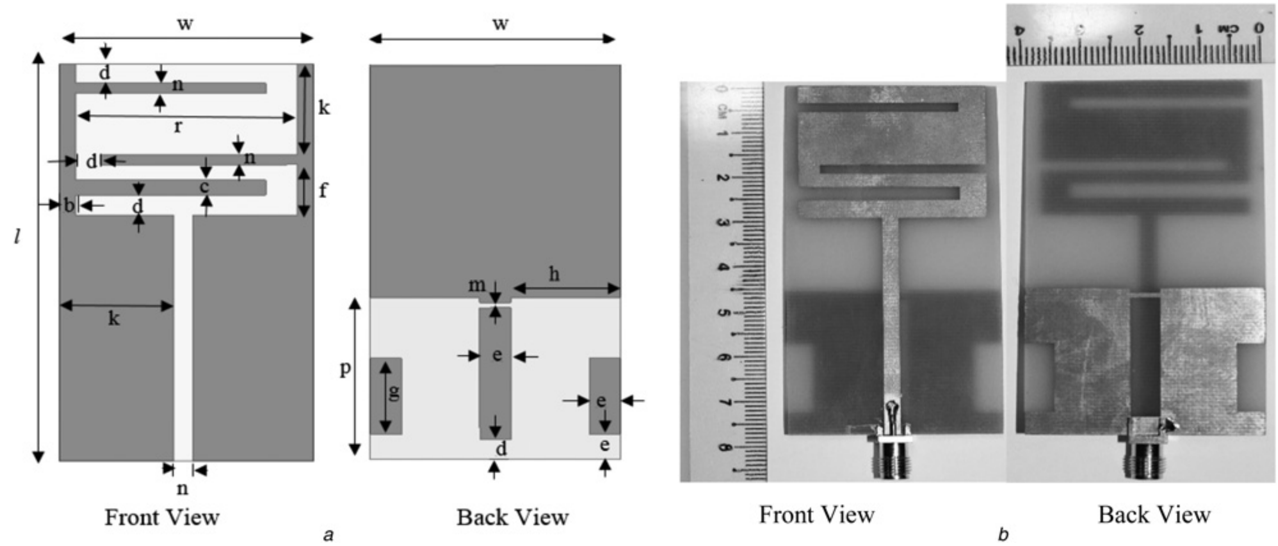

Fig. 1 *Geometry of proposed antenna*

a Antenna design layout
b Fabricated prototype

Table 1 Antenna design specifications

Parameters	Value, mm	Parameters	Value, mm
m	1	*g*	15
n	2	*h*	17
b	2.5	*k*	18
c	3	*p*	32
d	4	*r*	35
e	5	*w*	40
f	10	L	78

antenna are listed in Table 1. The radiating patch, ground plane, and microstrip transmission line are made of 0.035 mm thicken copper layer. The sub-miniature version A 50 Ω connector is utilised between the end of microstrip line and ground plane. The initial design analysis of the proposed antenna was performed in Microwave studio (MWS) of Computer Simulation Technology (CST) design environment [19]. Fig. 1*b* indicates the fabricated prototype of the proposed antenna, which is used for the measurement purpose in an anechoic chamber. The prototype was fabricated using printed copper layers on FR-4 substrate.

3 Models and methods

To determine the interaction between EM sources and the cell phone user, the dielectric properties of human body tissues should be set carefully. In this paper, a numerical specific anthropomorphic mannequin (SAM) head model [20] and a hand phantom are utilised as cell phone user's head and hand. The SAM phantom consists of shell and brain simulating liquid. As the human tissue parameters are frequency dependent, the dispersive material model is considered in the simulation of the cell phone with the head and hand phantom. Table 2 indicates the dielectric properties of head and hand phantom. A plastic casing box is used as a cover of

Table 2 Properties of head and hand models

Materials	Relative permittivity, ε_r		Conductivity, σ, S/m	
	900, MHz	1900, MHz	900, MHz	1900, MHz
SAM shell	3.7	3.5	0.0016	0.0016
SAM liquid	40.5	40	0.97	1.42
Hand	36.2	32.6	0.79	1.26

antenna in the experimental simulations with head and hand to take actual handset effect. An LCD screen of thickness 2.2 mm and a keyboard are used on the front side for mobile phone. The case box dimension is 82 mm × 42 mm × 8 mm. The dimensions and properties of handset components were set to comply with industrial standard.

The CST MWS based on finite-integral time-domain technique is utilised in this investigation. The simulation is carried out using time-domain solver considering hexahedral mesh with adaptive meshing scheme. Fig. 2 indicates the mobile phone model with head and hand in a cheek position of talk mode [21]. The power absorption by the mobile phone user can be evaluated from the induced electric field ($\boldsymbol{E}$) in the human biological tissue. Formulas (1) and (2) are used to evaluate the total absorbed power and the SAR, respectively [22]

$$P_{\text{abs}} = \frac{1}{2}\int_V \sigma|\boldsymbol{E}|^2 \mathrm{d}V \tag{1}$$

$$\text{SAR} = \frac{\sigma|\boldsymbol{E}|^2}{\rho} \tag{2}$$

where σ and ρ are the conductivity and density of mobile phone user's body tissue, respectively. The SAR values are calculated in the post-possessing phase of simulation according to the IEEE standard algorithm [23]. The peak SAR values (spatial-peak SAR [IEEE-1529]) were averaged over 1 and 10 g of human tissues by setting excitation equal to 0.6 W.

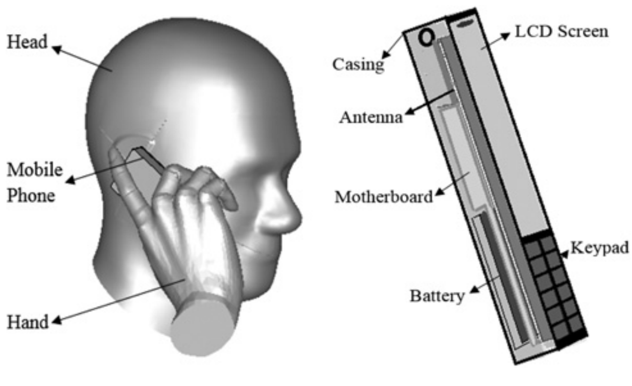

Fig. 2 *Simulation setup of mobile phone with head and hand*

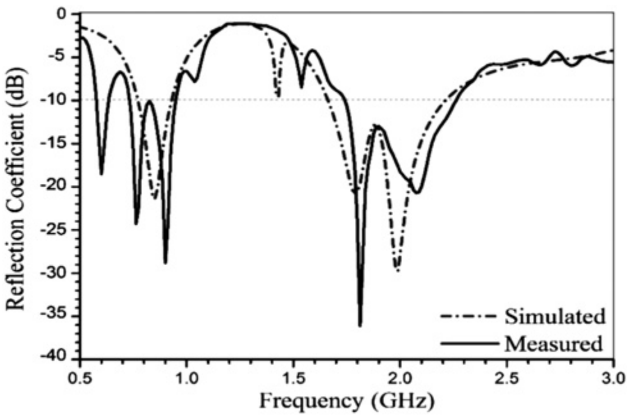

Fig. 3 *Reflection parameter (S_{11}) of proposed antenna*

4 Free-space antenna performances

In this section, the antenna performances are presented considering free-space condition. Fig. 3 presents the simulated and measured reflection parameter (S_{11}) for the proposed antenna. The presented measured results show that the antenna has an impedance bandwidth 230.4 MHz (0.725–0.95 GHz, lower band), and 522.24 MHz (1.74–2.25 GHz, upper band), which can cover GSM 900, DCS 1800, PCS 1900, GSM 1900, and UMTS 2100 MHz bands. To gain a better understanding of antenna performances, current distributions of antenna comprising radiator and ground plane are examined. The simulated current distributions of the proposed antenna are presented in Figs. 4*a–d* at 0.9, 1.8, 1.9, and 2.1 GHz, respectively. The final dimensions of the antenna are chosen from the fact that the antenna can comply with modern handset size. Fig. 5 indicates the measured gain radiation pattern of the proposed antenna at 0.9, 1.8, 1.9, and 2.1 GHz frequencies for GSM, DCS, PCS, and UMTS bands, respectively.

The results show near omnidirectional radiation patterns in the *x–y* plane. The measurement of radiation pattern, gain, and radiation efficiency is performed in an anechoic chamber at all frequencies. Results at other frequencies of the GSM, DCS, PCS, and UMTS bands exhibit very similar patterns as plotted, indicating stable radiation patterns are obtained. The radiation patterns of the proposed antenna are quite similar to the planar quarter-wavelength mono-pole antenna. The measured radiation efficiencies at targeted frequencies (0.9, 1.8, 1.9, and 2.1 GHz) show values larger than 88%. The measured isotropic peak gain of the proposed antenna is varied from 2 to 2.58 dBi at different frequency bands. More specifically, 2, 2.14, 2.51, and 2.58 dBi gains are obtained at 0.9, 1.8, 1.9, and 2.1 GHz, respectively.

5 User effects on antenna

In this investigation, antenna performances are presented using three different configurations comprising antenna in free space, antenna with head phantom and antenna with both head and hand phantom. The antenna performances with user phantoms can give an approximate idea of real use of the antenna. Fig. 6 represents the simulation results of the reflection parameter (S_{11}) of the proposed antenna for three different configurations. The inclusion of user phantoms (head and hand) detune the resonance frequencies of antenna due to the higher dielectric properties of human tissues. The results show that the antenna with both head and hand leads impedance mismatch significantly at the upper frequency bands. Figs. 7*a* and *b* indicate the peak radiation efficiencies and peak directivities of the proposed antenna in a column chart at 0.9 GHz, 1.8 GHz, 1.9 MHz, and 2.1 GHz considering for three different configurations. The results indicate that the inclusion of user phantoms reduces the radiation efficiencies and increases the directivities of antenna. For free-space configuration, antenna radiation efficiencies are 98, 89, 94, and 98% at 0.9, 1.8, 1.9, and 2.1 GHz, respectively. The results of antenna with head configuration indicate ~45% reduction of radiation efficiencies for all the frequencies due to the effects of user's head. In addition, antenna with head and hand configuration produces further 20% (approximately) reduction of radiation efficiencies for all frequencies. As the directivity radiation patterns are not identical for different frequencies of exposure and configurations (i.e. free space, with head, and with head–hand), corresponding angles (theta and phi) for values of peak directivity vary for different frequencies and configurations. Moreover, the corresponding angles for each value of peak directivity and radiation efficiency of Fig. 7 are included in Table 3. In case of antenna with human phantoms analysis, the radiation characteristics of antenna are changed due to several factors such as absorption loss, impedance mismatch, and reflection back of available power [24]. This is happened due to the high dielectric properties of human tissues. The proposed antenna radiation pattern is nearly omnidirectional in free-space condition. In case of head configuration, the radiation in the direction of the human head is prevented and a significant amount is reflected away from the human head [25]. Thus, an increase in directivity is observed in the direction opposite to the human head. Moreover, the hand phantom also strongly affects antenna

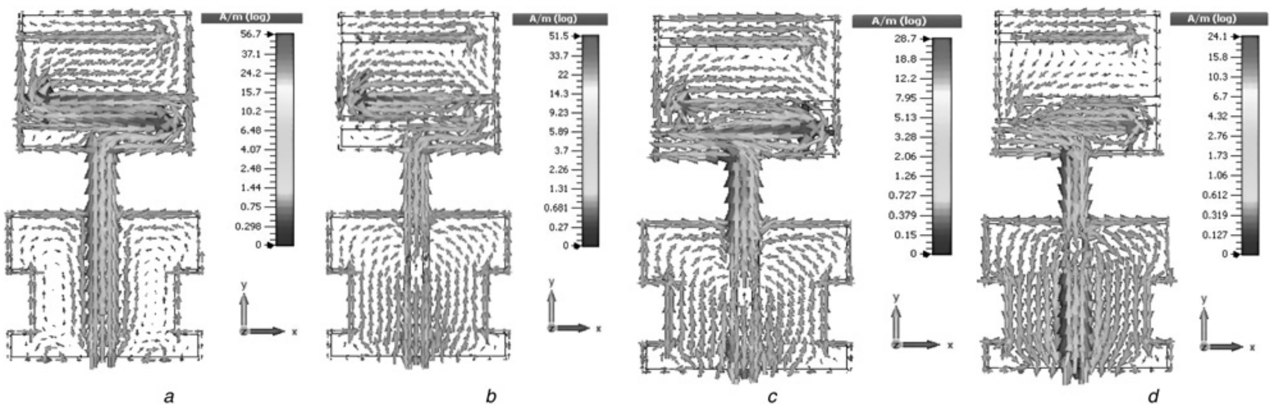

Fig. 4 *Simulated surface current (J_{surf}) distribution of antenna at*

a 0.9 GHz
b 1.8 GHz
c 1.9 GHz
d 2.1 GHz

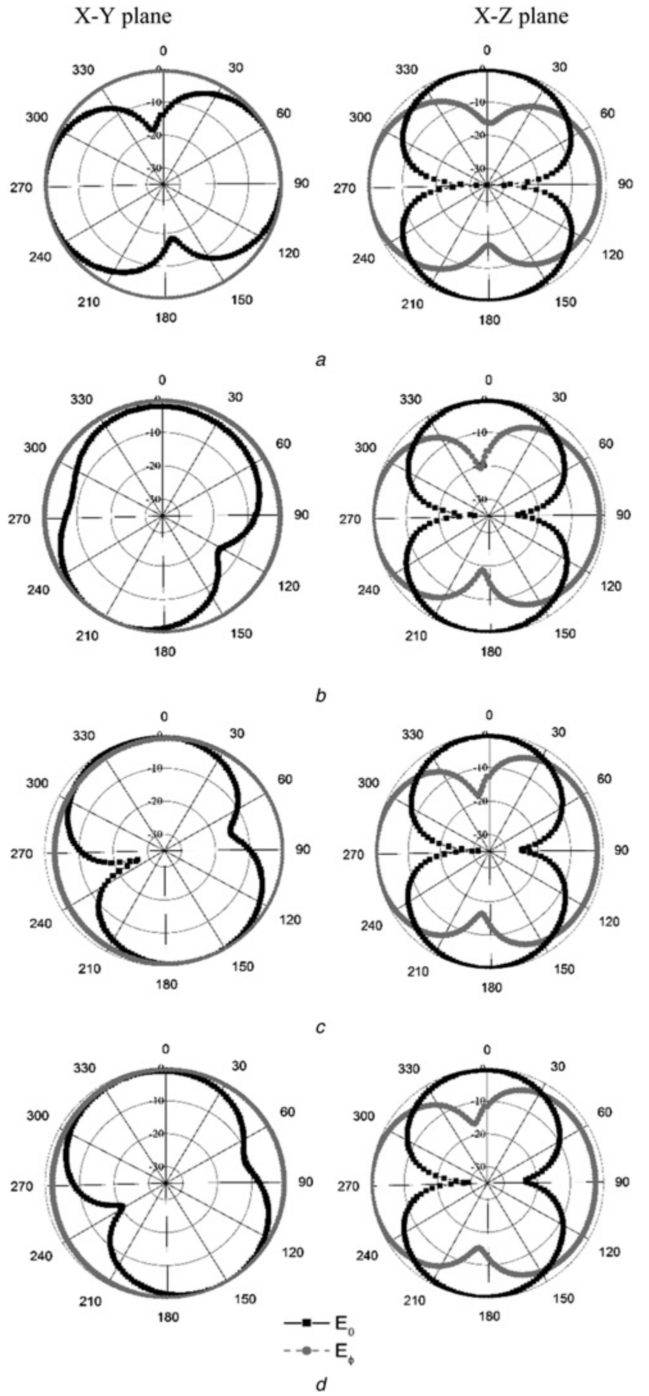

Fig. 5 *Measured gain radiation pattern of the proposed antenna*

a 900 MHz
b 1800MHz
c 1900MHz
d 2100 MHz

radiation characteristics [26]. In case of antenna with head–hand configuration, it contributes further power absorption and reflection which results in decay in directivity. Beside the general trends, an increment in directivity is observed in the antenna with head–hand at 900 MHz compared with head configuration. In some cases, it is possible that the hand phantom may lead to increase in antenna performances [27]. As reported in [28], involving hand phantom has positive impact on handset antenna (i.e. increase in antenna performances) for lower frequency band (900 MHz and lower frequencies). At the lower frequencies, hand phantom enlarge ground plane effects effectively which leads to increase in directivity.

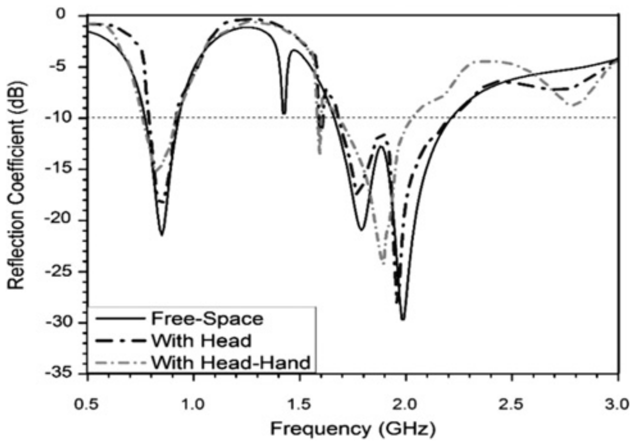

Fig. 6 *Reflection parameters (S_{11}) of proposed antenna comprising free space, with head and with both head and hand*

The directivity radiation patterns of the proposed antenna comprising free space, with head, and with head–hand configurations are shown in Figs. 8*a*–*d* at 0.9, 1.5, 1.8, and 1.9 GHz, respectively. The radiation patterns are plotted varying both θ and ϕ angle and corresponding magnitude of directivity is indicated using colour variation. The user's phantoms lead to change the free-space radiation pattern and increase directivity. The antenna directivities are increased greatly from free space to head configurations. In addition, the antenna with both head and hand configuration leads further moderate increment in directivities than that with head configuration.

6 SAR analysis

The SAR values of the proposed antenna are evaluated considering cheek position of talk mode of the mobile phone. In the SAR evaluation set-up, the antenna is placed using two orientations: the first one, in which the antenna patch (front part) is placed against the head and upper portion (top position), and the other one, in which the antenna is rotated 180° (bottom position). The 10 g SAR values along with three-dimensional distribution of SAR of the proposed antenna are presented in Fig. 9. The SAR results for the top patch position are a little bit lower than that of the bottom patch positions. The SAR value shows variation at different frequency bands as the radiated power of the antenna is not identical at different frequency bands. The obtained 10 g SAR values for the proposed antenna are below the maximum SAR limit. The SAR values of the proposed microstrip-patch antenna are compared with the SAR values of three other common antennas: dipole antenna, helical antenna, and PIFA at 0.9 GHz. The half-wave dipole and single-band helical antenna are designed to operate at 0.9 GHz and tested under similar conditions of the proposed patch antenna. A dual-band PIFA is designed, which operates at 0.9 and 1.8 GHz. The comparison of SAR values is presented at 0.9 GHz frequency only. The SAR values (1 and 10 g) are plotted in Fig. 10 for half-wave dipole, helical, PIFA, and

Table 3 Corresponding angles of peak directivity for different configurations

Frequency, GHz	Angles (θ, ϕ in deg)		
	Free space	With head	With head–hand
0.9	70, 350	0, 10	15, 255
1.8	115, 335	10, 115	10, 235
1.9	115, 5	5, 65	35, 50
2.1	160, 345	5, 170	35, 40

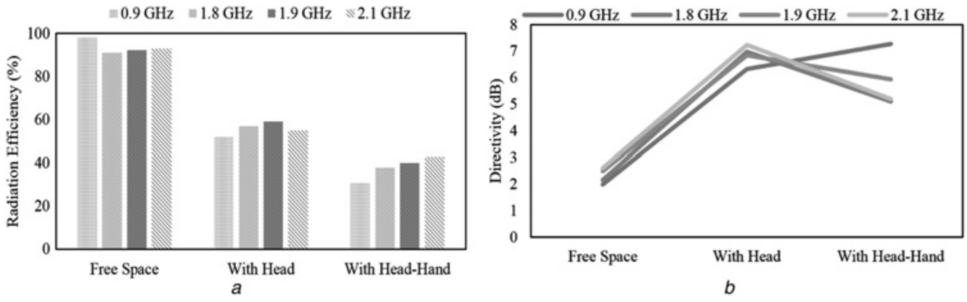

Fig. 7 *Proposed antennas at 0.9, 1.5, 1.8, and 1.9 GHz*

a Radiation efficiencies
b Directivities

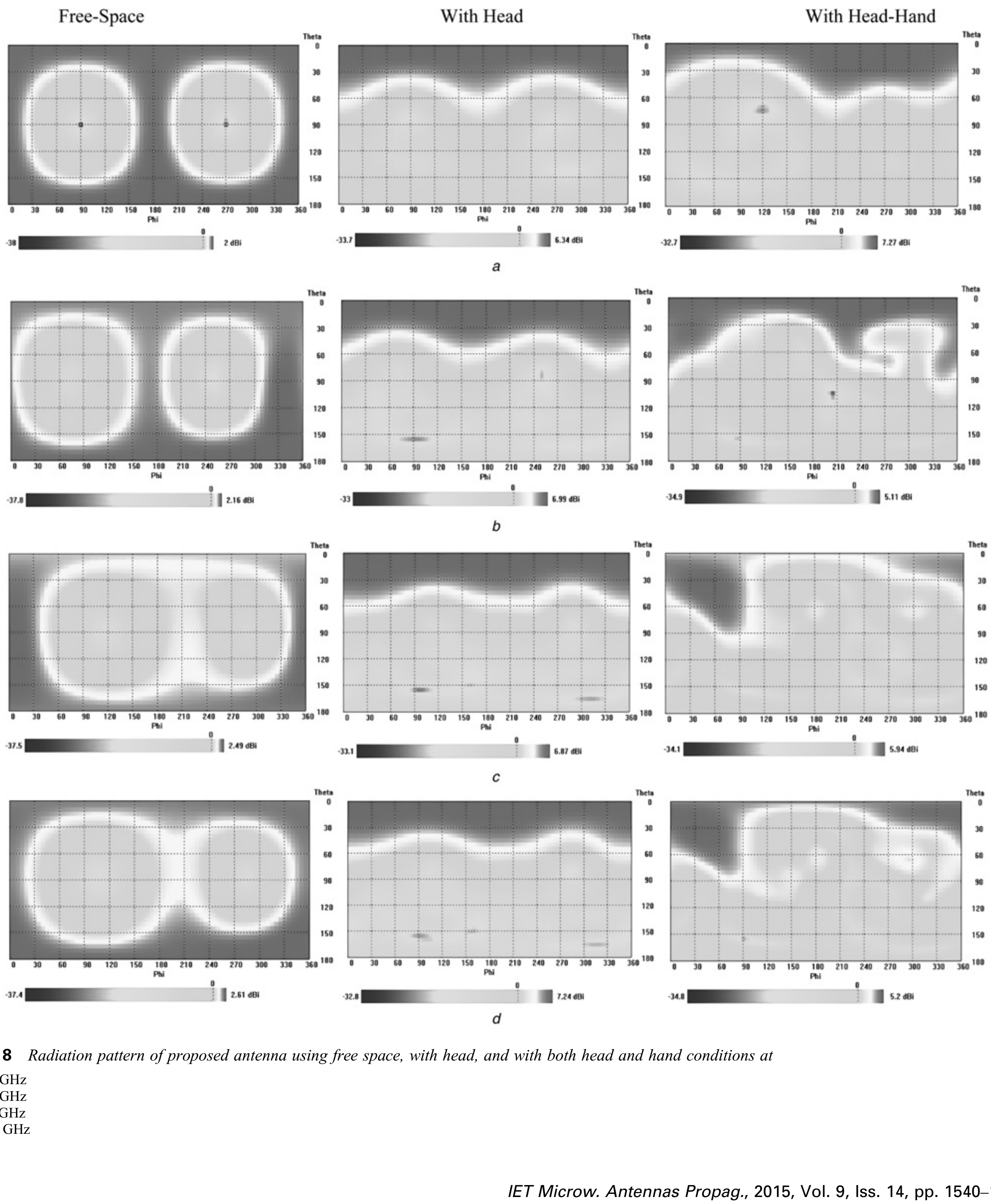

Fig. 8 *Radiation pattern of proposed antenna using free space, with head, and with both head and hand conditions at*

a 0.9GHz
b 1.8GHz
c 1.9GHz
d 2.1 GHz

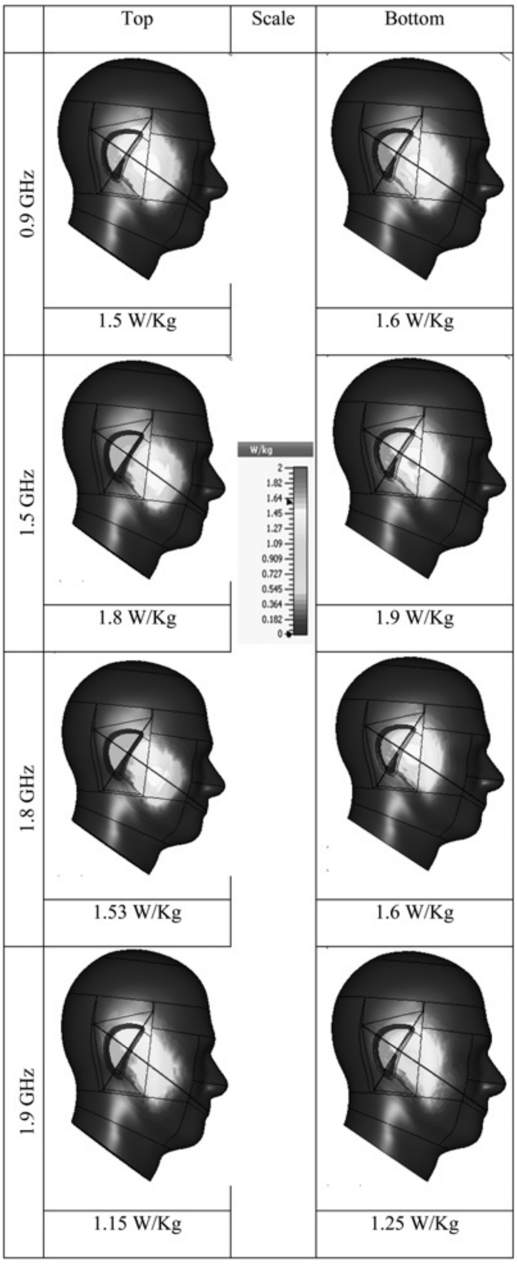

Fig. 9 *10 g SAR values of proposed antenna*

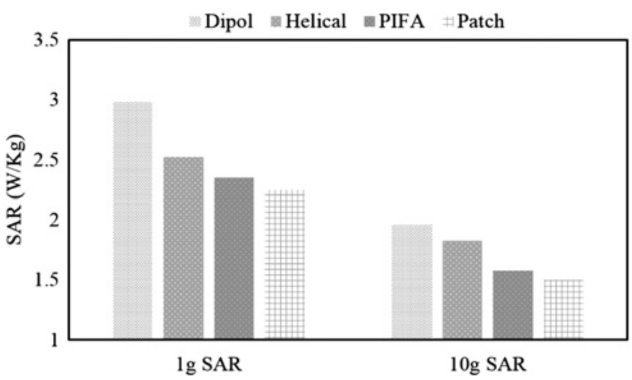

Fig. 10 *SAR comparison of dipole, helical, PIFA, and proposed patch antenna*

proposed microstrip-patch antenna. At 0.9 GHz, the proposed antenna produces 2.25 1 g SAR and 1.5 10 g SAR, which are considerably lower than that of a PIFA, dipole, and helical antenna.

7 Conclusion

In this article, a new microstrip-patch antenna is introduced for modern cellular phone applications. The proposed antenna successfully covers four different frequency bands comprising GSM, DCS, PCS, and UMTS. Moreover, the antenna can maintain desired frequency bands in a real user environment with head and hand. The SAR values of the proposed antenna are below the maximum SAR limit. In addition, the comparative analysis of the proposed antenna with dipole antenna, helical antenna, and PIFA clearly shows the low-power absorption characteristics of the proposed antenna in the human head.

8 References

1 Elsadek, H.: 'Microstrip antennas for mobile wireless communication systems' (INTECH Open Access Publisher, 2010), pp. 163–190

2 Abutarboush, H.F., Nilavalan, R., Peter, T., Cheung, S.W.: 'Multiband inverted-F antenna with independent bands for small and slim cellular mobile handsets', *IEEE Trans. Antennas Propag.*, 2011, **59**, (7), pp. 2636–2645

3 Kuo, Y.-L., Wong, K.-L.: 'Coplanar waveguide-fed folded inverted-F antenna for UMTS application', *Microw. Opt. Technol. Lett.*, 2002, **32**, (5), pp. 364–366

4 Peng, C.-M., Chen, I.-F., Chien, C.-T.: 'A novel hexa-band antenna for mobile handsets application', *IEEE Trans. Antennas Propag.*, 2011, **59**, (9), pp. 3427–3432

5 Du, Y., Zhao, A.: 'An internal quad-band antenna for oval-shaped mobile phones', *IEEE Antennas Wirel. Propag. Lett.*, 2010, **9**, pp. 830–833

6 Sittironnarit, T., Ali, M.: 'Analysis and design of a dual-band folded microstrip patch antenna for handheld device applications', Proc. IEEE SoutheastCon, Columbia, SC, April 2002, 2002, pp. 255–258

7 Paul, B., Mridula, S., Aanandan, C.K., Mohanan, P.: 'A new microstrip patch antenna for mobile communications and Bluetooth applications', *Microw. Opt. Technol. Lett.*, 2002, **33**, (4), pp. 285–286

8 Lin, S.-Y., Huang, K.-C.: 'A compact microstrip antenna for GPS and DCS application', *IEEE Trans. Antennas Propag.* , 2005, **53**, (3), pp. 1227–1229

9 Costantine, J., Kabalan, K.Y., El-Hajj, A., Rammal, M.: 'New multi-band microstrip antenna design for wireless communications', *IEEE Antennas Propag. Mag.*, 2007, **49**, (6), pp. 181–186

10 Jhamb, K., Li, L., Rambabu, K.: 'Novel-integrated patch antennas with multi-band characteristics', *IET Microw. Antennas Propag.*, 2011, **5**, (12), pp. 1393–1398

11 Samsuzzaman, M., Islam, T., Abd Rahman, N.H., Faruque, M.R.I., Mandeep, J.S.: 'Coplanar waveguide fed compact wide circular-slotted antenna for Wi-Fi/WiMAX applications', *Int. J. Antennas Propag.*, 2014, **2014**, 10pp., article ID 982958,doi: 10.1155/2014/982958

12 Hossain, M.I., Faruque, M.R.I., Islam, M.T.: 'Analysis on the effect of the distances and inclination angles between human head and mobile phone on SAR', *Prog. Biophys. Mol. Biol.*, 2015, article in press, doi: 10.1016/j.pbiomolbio.2015.03.008

13 'WHO|Electromagnetic fields and public health: mobile phones'. Available at http://www.who.int/mediacentre/factsheets/fs193/en/, accessed October 2014

14 'IEEE standard for safety levels with respect to human exposure to radio frequency electromagnetic fields, 3 kHz–300 GHz–amendment 1: specifies ceiling limits for induced and contact current, clarifies distinctions between localized exposure and spatial peak power density', IEEE Std C951a-2010 Amend. IEEE Std C951-2005, 2010, pp. C1–C9

15 Guideline, I.: 'Guidelines for limiting exposure to time-varying electric, magnetic, and electromagnetic fields (up to 300 GHz)', *Health Phys.*, 1998, **74**, (4), pp. 494–522

16 Commission F.C., others: 'Evaluating compliance with FCC guidelines for human exposure to radiofrequency electromagnetic fields'. Tech. Rep. Suppl. C to OET Bulletin 65, FCC, Washington, DC, 2001), pp. 1–48

17 Pelosi, M., Franek, O., Knudsen, M.B., Pedersen, G.F., Andersen, J.B.: 'Antenna proximity effects for talk and data modes in mobile phones', *IEEE Antennas Propag. Mag.*, 2010, **52**, (3), pp. 15–27

18 Guo, Q., Mittra, R., Lei, F., Li, Z., Ju, J., Byun, J.: 'Interaction between internal antenna and external antenna of mobile phone and hand effect', *IEEE Trans. Antennas Propag*, 2013, **61**, (2), pp. 862–870

19 'CST MICROWAVE STUDIO–3D EM simulation software'. Available at https://www.cst.com/Products/CSTMWS, accessed November 2014

20 Panagamuwa, C.J., Whittow, W.G., Edwards, R.M., Vardaxoglou, J.C.: 'Experimental verification of a modified specific anthropomorphic mannequin (SAM) head used for SAR measurements'. Antennas and Propagation Conf., 2007. LAPC 2007, Loughborough, April 2007, pp. 261–264

21 Faruque, M.R.I., Husni, N.A., Islam, M.T., Misran, N.: 'Effects of mobile phone radiation onto human head with variation of holding cheek and tilt positions', *J. Appl. Res. Technol.*, 2014, **12**, (5), pp. 871–876

22 Hwang, J.-N., Chen, F.-C.: 'Reduction of the peak SAR in the human head with metamaterials', *IEEE Trans. Antennas Propag.*, 2006, **54**, (12), pp. 3763–3770

23 IEEE: 'Recommended practice for determining the peak spatial-average specific absorption rate (SAR) in the human head from wireless communications devices: measurement techniques', IEEE Standard 1528–2003, 2003

24 Pelosi, M., Franek, O., Knudsen, M.B., Pedersen, G.F., Andersen, J.B.: 'Antenna proximity effects for talk and data modes in mobile phones', *IEEE Antennas Propag. Mag.*, 2010, **52**, (3), pp. 15–27

25 Liu, P., Perovic, N.S., Springer, A.: 'The impact of user effects on the performance of dual receive antenna diversity systems in flat Rayleigh fading channels', *Radioengineering*, 2014, **23**, (1), pp. 286–299
26 Holopainen, J., Poutanen, J., Icheln, C., Vainikainen, P.: 'User effect of antennas for handheld DVB terminal'. Int. Conf. on Electromagnetics in Advanced Applications, Torino, Sept. 2007. ICEAA 2007, 2007, pp. 496–499
27 Holopainen, J., Kivekas, O., Ilvonen, J., Valkonen, R., Icheln, C., Vainikainen, P.: 'Effect of the user's hands on the operation of lower UHF-band mobile terminal antennas: focus on digital television receiver', *IEEE Trans. Electromagn. Compat.*, 2011, **53**, (3), pp. 831–841
28 Hui, P.: 'Positive hand effects on mobile handset antennas', Microwave Conf., Macau, Dec. 2008, APMC 2008. Asia-Pacific, 2008, pp. 1–4